Elsevier Editorial System(tm) for Carbohydrate Polymers

Manuscript Draft

Manuscript Number:

Title: Nanostructured starch combined with hydroxytyrosol in poly(vinyl) alcohol based ternary films as novel food active packaging solutions

Article Type: Research Paper

Keywords: poly(vinyl alcohol) (PVA); hydroxytyrosol; starch nanocrystals; starch nanoparticles; food active packaging; antioxidant properties.

Corresponding Author: Professor Luigi Torre, PhD

Corresponding Author's Institution: University of Perugia

First Author: Francesca Luzi

Order of Authors: Francesca Luzi; Elena Fortunati; Alessandro Di Michele; Elisa Pannucci; Ermelinda Botticella; Luca Santi; Josè M Kenny; Luigi Torre, PhD; Roberta Bernini

Abstract: Novel ternary films have been realized by using poly(vinyl alcohol) (PVA) as polymeric matrix, nanostructured starch as reinforcement phase and hydroxytyrosol (HTyr), a low-molecular phenolic compound present in olive oil, as antioxidant agent. Nanostructured starch, in the form of starch nanocrystals (NC) and nanoparticles (NP) obtained by acid hydrolysis and ultrasound irradiation of starch derived from the bread wheat variety Cadenza (WT, amylose content 33%) and a derived-high amylose line (HA, amylose content 75%), was considered. The developed multifunctional films (named PVA/NCWT/HTyr, PVA/NCHA/HTyr, PVA/NPWT/HTyr, PVA/NPHA/HTyr) were characterized in terms of morphological, thermal and optical properties, water absorption capacity, overall and specific migration into a food simulant and antioxidant properties. Experimental data showed that HTyr was released in a controlled manner from all ternary films and the released HTyr still retained a strong antioxidant activity. The release profiles, compared to those of PVA/HTyr binary films, demonstrated the key role of nanostructured starch in the ternary formulations in promoting a controlled release of HTyr. Overall, PVA/NPWT/HTyr resulted as the most promising ternary formulation for food packaging applications.

Suggested Reviewers: Amalia Cano Embuena
Instituto de Ingeniería de Alimentos para el Desarrollo, Universitat Politècnica de València
amcaem@upvnet.upv.es
She is and expert in the food packaging sector

Weijun Yang
Institute of Earth and Environmental Sciences, Freiburg Materials Research Center (FMF)
weijun.yang2012@gmail.com
He is an expert in the field of antioxidant ingredients in polymeric matrices

Marina Ramos
Analytical Chemistry, Nutrition and Food Sciences Department, University of Alicante
marina.ramos@ua.es
She is an expert in the field of active ingredient release in polymers

**UNIVERSITY OF PERUGIA**
Faculty of Engineering
Department of Civil and Environmental Engineering

*Luigi Torre, Prof.*
*Materials Science and Technology - European Centre for Nanostructured Polymers*

Terni, 22/12/2017

Editorial Board

Carbohydrate Polymers

Dear Editor,

Please find enclosed the manuscript entitle "**Nanostructured starch combined with hydroxytyrosol in poly(vinyl) alcohol based ternary films as novel food active packaging solutions**" by Francesca Luzi, Elena Fortunati, Alessandro Di Michele, Elisa Pannucci, Ermelinda Botticella, Luca Santi, José Maria Kenny, Luigi Torre, Roberta Bernini, that I would like to submit for possible publication in Carbohydrate Polymers

In the present work, we have realized novel ternary films by using poly(vinyl alcohol) (PVA) as polymeric matrix, nanostructured starch as reinforcement phase and hydroxytyrosol (HTyr), a low-molecular phenolic compound present in olive oil, as antioxidant agent. Nanostructured starch, in the form of starch nanocrystals (NC) and nanoparticles (NP) obtained by acid hydrolysis and ultrasound irradiation of starch derived from two varieties (WT, amylose content 33% and HA, a high amylose line, 75%) was considered. Results of morphological, thermal and optical properties, water absorption capacity, overall and specific migration into a food simulant and antioxidant properties for the developed multifunctional films proved that HTyr was released in a controlled manner from all ternary films and the released HTyr still retained a strong antioxidant activity. The release profiles, compared to those of PVA/HTyr binary films, demonstrated the key role of nanostructured starch in the ternary formulations in promoting a controlled release of HTyr. Overall, PVA/$NP_{WT}$/HTyr resulted as the most promising ternary formulation for food packaging applications.

I declare that all the authors mutually agree that it should be submitted to CARBPOL, that this is the original work of the authors and that the manuscript was not previously submitted to CARBPOL.

I look forward to receiving your comments at your earliest convenience.

Sincerely,

Prof. Luigi Torre

Strada di Pentima 4 – 05100 Terni – Tel. (39) 0744 492918 - email: luigi.torre@unipg.it

## Highlights

1. Nanostructured starch (nanocrystals (NC) and nanoparticles (NP)) were obtained by acid hydrolysis and ultrasound irradiation.
2. Starch with amylose content 33% (WT) and a derived-high amylose line (HA, amylose content 75%), were considered.
3. Solvent cast films were prepared including hydroxytyrosol (HTyr) and starch nanostructures into PVA.
4. Nanostructured starch in ternary formulations promoted a controlled release of HTyr and a tuned antioxidant activity.

# Nanostructured starch combined with hydroxytyrosol in poly(vinyl) alcohol based ternary films as novel food active packaging solutions

Francesca Luzi[a], Elena Fortunati[a], Alessandro Di Michele[b], Elisa Pannucci[c], Ermelinda Botticella[c], Luca Santi[c], José Maria Kenny[a], Luigi Torre[a*], Roberta Bernini[c]

[a] *University of Perugia, Civil and Environmental Engineering Department, Strada di Pentima 4, 05100 Terni (Italy)*

[b] *University of Perugia, Physic and Geology Department, Via Pascoli, 06123 Perugia (Italy)*

[c]*University of Tuscia, Department of Agricultural and Forestry Sciences (DAFNE), Via S. Camillo De Lellis, 01100 Viterbo, (Italy)*

[*]**Corresponding author**: Luigi Torre, Strada di Pentima 4, 05100 Terni (I), Tel.: +39-0744492918; fax: +39-0744492950; E-mail address: luigi.torre@unipg.it.

## Abstract

Novel ternary films have been realized by using poly(vinyl alcohol) (PVA) as polymeric matrix, nanostructured starch as reinforcement phase and hydroxytyrosol (HTyr), a low-molecular phenolic compound present in olive oil, as antioxidant agent. Nanostructured starch, in the form of starch nanocrystals (NC) and nanoparticles (NP) obtained by acid hydrolysis and ultrasound irradiation of starch derived from the bread wheat variety Cadenza (WT, amylose content 33%) and a derived-high amylose line (HA, amylose content 75%), was considered. The developed multifunctional films (named PVA/$NC_{WT}$/HTyr, PVA/$NC_{HA}$/HTyr, PVA/$NP_{WT}$/HTyr, PVA/$NP_{HA}$/HTyr) were characterized in terms of morphological, thermal and optical properties, water absorption capacity, overall and specific migration into a food simulant and antioxidant properties. Experimental data showed that HTyr was released in a controlled manner from all ternary films and the released HTyr still retained a strong antioxidant activity. The release profiles, compared to those of PVA/HTyr binary films, demonstrated the key role of nanostructured starch in the ternary formulations in promoting a controlled release of HTyr. Overall, PVA/$NP_{WT}$/HTyr resulted as the most promising ternary formulation for food packaging applications.

**Keywords:** poly(vinyl alcohol) (PVA), hydroxytyrosol, starch nanocrystals, starch nanoparticles, food active packaging, antioxidant properties.

## 1. Introduction

A recent study carried out from the Food and Agriculture Organization of the United Nations (FAO) reported that every year about one-third of food produced for human consumption, consisting in about 1.3 billion tons, is globally wasted or lost (http://www.fao.org/news/story/it/item/196458/icode;http://www.fao.org/docrep/018/i3347e/i3347e.pdf). These data are alarming in many respects: first from an ethical point of view, because more than 870 million people worldwide are suffering from hunger; secondly from an economic point of view, because this represents a loss of 750 billion dollars every year; and finally, from an environmental point of view, because food production has an impact on climate, soil and biodiversity even if food is not consumed.

In this scenario, all strategies aiming to maximise the amount of food available for human consumption, to minimise the environmental burden, to reduce the economic impact and to improve food safety are encouraged. Among them, the measures focused on food preservation play an important role. Food preservation consists in preventing all aspects involved in food deterioration which ultimately are cause of loss in nutritional value and safety of food. Among these, the most relevant are the oxidative processes, which are responsible, for example, for degradation of vitamins, for alteration of flavour and for visual deterioration of food such as the browning of fruits, vegetables and meat. In this respect, food active packaging solutions represent strategies spanning through the entire food chain from producers and distributors to consumers (Lee, Lee, Choi, & Hur, 2015). In fact, polymeric films used to prepare food packaging, can incorporate ingredients active in preventing degradations by slowing down such processes. Recently, several phenolic compounds (Agustin-Salazar, Gamez-Meza, Medina-Juàrez, Soto-Valdez, & Cerruti, 2014; Castro López, López de Dicastillo, López Vilariño, & González Rodríguez, 2013) and natural extracts (Ambrogi et al., 2011; Cerruti, Malinconico, Rychly, Matisova-Rychla, & Carfagna, 2009) have been investigated for this purpose and, in this respect, we selected and reported on the use of hydroxytyrosol (HTyr), a natural low-molecular phenol present in olive oil, olive leaves and olive oil by-products (Bernini, Merendino, Romani, & Velotti, 2013; Gambacorta, Tofani, Bernini, & Migliorini, 2007; Romani, Pinelli, Ieri, & Bernini, 2016) and hydroxytyrosol methyl carbonate (HTyr-MC), a synthetic HTyr-derived compound (Bernini et al., 2017; Bernini, Gilardini Montani, Merendino, Romani, & Velotti, 2015), both known for their potent antioxidant activity. In particular, we successfully developed a panel of binary formulations based on poly(vinyl alcohol) (PVA) incorporating HTyr or HTyr-MC by solvent casting method (Fortunati, Luzi, Dugo, et al.,

2016; Fortunati, Luzi, Fanali, et al., 2016). These films appeared homogeneous and the overall migration levels of each active ingredient were lower than the migration limits permitted by the current legislation for food contact materials (European, 2011). In addition, antioxidants assays performed on the HTyr and the HTyr-MC released from the binary films into a hydrophilic food simulant offered a clear evidence of strong activity. However, in both cases their release from the films was not carried out in a controlled fashion but reproducibly reached the maximum level the first day of contact, thus representing a considerable limitation for food packaging applications.

Over the last decades, nanostructured materials have been intensely investigated for improving drug delivery and films performances in industrial applications (Domingues et al., 2015; Luzi et al., 2016; Stark, Stoessel, Wohlleben, & Hafner, 2015; Wang et al., 2015). As a matter of fact, the nanometric size grants to these materials a greater surface area per mass and this feature may permit a slower and thus more controlled release of an active ingredient from a film matrix (Acevedo-Fani, Soliva-Fortuny, & Martín-Belloso, 2016; Siró et al., 2006).

Among the possible polymers suitable for the production of nanomaterials, our attention has been turned on starch, a natural, renewable and biodegradable polymer. Structurally, it consists of two macromolecules, amylose and amylopectin. Amylose is a linear polymer of α-D-glucose units linked by α-1,4-glycosidic bonds; amylopectin is a highly branched polymer consisting of α-D-glucose units linked by α-1,4-glycosidic bonds and α-D-glucose units by α-1,6-glycosidic bonds. The ratio of these two polymers is generally related to the botanic origin of starch (LeCorre, Bras, & Dufresne, 2011) and in turn is responsible for the shape, size and crystalline organization of starch granules.

In this light, with the objective of developing novel ternary multifunctional films for food active packaging that could perform a release of the antioxidant (HTyr) in a controlled manner, we included, by solvent casting technique, starch nanocrystals (NC) or starch nanoparticles (NP) into the PVA film matrix. In particular, for the preparation of the two types of nanostructures, we used starch extracted from the bread wheat variety Cadenza (WT, amylose content 33%) and from a derived-high amylose line (HA, amylose content 75%) produced by Botticella et al (Botticella; E.; Sestili, F.; Sparla, F.; et al. Plant Biotech. J. submitted). All formulations, namely PVA/$NC_{WT}$/HTyr, PVA/$NC_{HA}$/HTyr, PVA/$NP_{WT}$/HTyr and PVA/$NP_{HA}$/HTyr, were investigated in terms of optical, morphological, thermal and mechanical properties. Moreover, in order to evaluate the kinetic of release of HTyr from each film, overall and specific migration tests were performed using a food simulant according to the current European legislation.

## 2. Experimental part

### 2.1 Materials

All chemicals including high purity grade poly(vinyl alcohol) (average $M_W$ 124-146 kg $mol^{-1}$, 99% hydrolyzed) were purchased by Sigma-Aldrich® (Italy). Silica gel 60 F254 plates and silica gel 60 (230-400 mesh) were provided by Merck (Germany).

### 2.2 HTyr synthesis and characterization

HTyr was synthesized according to a procedure already optimized by Bernini et al. (Bernini, Mincione, Barontini, & Crisante, 2008; Bernini et al., 2007) and characterized by proton and carbon nuclear magnetic resonance using a 400 MHz Spectrometer Avance III (Bruker, Germany).

### 2.3 Starch extraction

Starch was obtained from the bread wheat variety Cadenza (WT, amylose content 33%) and from a derived high amylose line (HA, amylose content 75%) as described by Botticella et al (Botticella; E.; Sestili, F.; Sparla, F.; et al. Plant Biotech. J. submitted). Briefly, starch was isolated from whole flour of the WT and HA wheats by the dough ball method (Wolf, M. (1964). 50 g of whole flour were mixed with 60% of water and hand kneaded until optimal dough development. Starch was washed from the dough with water (300 mL) and, after centrifugation at 1500 rpm, the starch pellet was washed twice with 20 mL of water. The thin yellow-gray layer deposited on the surface of the starch pellet was scraped off by a spatula. Starch pellet was subsequently let to dry for two days at 25 °C.

### 2.4 Starch nanocrystal synthesis and characterization

Starch granules, both WT or HA (25 g), were mixed with 200 mL of 3.16 M sulfuric acid for 5 days at 40 °C, with a stirring speed of about 100 rpm as previously reported (Angellier, Choisnard, Molina-Boisseau, Ozil, & Dufresne, 2004). After the hydrolysis, the obtained suspension was diluted with distilled water, centrifuged (4000 rpm for 20 min) and filtered (filter mesh 2 µm) in order to eliminate residual unreacted material. The resultant starch nanocrystal aqueous suspensions were ultrasonicated by means of a tip sonicator (Vibracell, 750) for 10 min. The final yield for both WT and HA obtained starch nanocrystals was calculated as % of initial weight of the used raw material.

The obtained starch NC were characterized by Field Emission Scanning Electron Microscopy (FESEM) using a Field Emission Gun Electron Scanning Microscopy LEO 1525 (Zeiss); the morphology was observed after metallization with Cr.

X-ray powder diffraction (XRD: PANalytical X'Pert Pro, Cu Ka radiation) operating at 40 kV and 40 mA, step size 0.0170 2 h and step scan 20 s was used to evaluate the change in starch crystallinity in NC structures.

### 2.5 Starch nanoparticle synthesis and characterization

A high power ultrasound generator titanium horn type 750 W (VCX 750 Sonic and Materials), 20 kHz, with a tip diameter of 13 mm, was used for the synthesis of starch NP. 1 g of WT and 1 g of HA starch were placed in a fused bottle with 100 mL of pure water. The bottle was hermetically sealed to the horn and then subjected, for 50 minutes at 8 °C, under argon flow (100 mL/min), to high power ultrasound irradiation (50% amplitude). After ultrasonication, each colloid suspension was centrifuged at 4000 rpm for 20 min. The resulting concentration of the aqueous WT suspension was 0.13 mg/mL, while HA suspension was 0.35 mg/mL. The obtained starch NP were characterized by Field Emission Scanning Electron Microscopy (FESEM) and by XRD using the same procedure described above for NC characterization.

### 2.6 Preparation of the ternary formulations

PVA binary and ternary based formulations were prepared by solvent casting technique. The concentration of active HTyr was fixed at 5 wt% (concentration selected on the basis of previous results) (Fortunati, Luzi, Fanali, et al., 2016), while two different concentrations, 1 and 3 wt % of starch nanostructures (NC and NP), were selected for the preparation of binary based formulations (**Table 1**). The ternary based films were produced combining HTyr at 5 wt% and only one concentration of starch nanostructures, specifically 1 wt% (this concentration was selected on the base of results coming from PVA binary based formulations here reported). PVA based formulations were prepared by using the procedure described by Fortunati and co-authors (Fortunati, Luzi, Dugo, et al., 2016; Fortunati, Luzi, Fanali, et al., 2016). Firstly, 0.5 g of PVA was dissolved in 10 mL of distilled water under magnetic stirring for 2 h at 80 °C. The polymeric solution was kept under magnetic stirring to reach room temperature (RT).

PVA/HTyr was obtained mixing, under magnetic stirring, the polymeric solution with a specific amount of HTyr previously dispersed in distilled water (0.1 g of HTyr in 10 mL of distilled water)

for 1 h at RT. Uniform dispersion of HTyr in aqueous solution was obtained applying a magnetic stirring and a sonication bath, both at RT for 1 h. PVA/NC or PVA/NP were obtained mixing the amount of nanostructures in aqueous solution with polymeric aqueous suspensions under magnetic stirring for 1h at RT.

Ternary based formulations were obtained mixing firstly the amount of NC or NP with HTyr in aqueous suspension for 1 h at RT, to obtain an uniform dispersion of nanofillers and active ingredient, then the obtained solution was added to PVA. PVA/HTyr/NC or PVA/HTyr/NP in aqueous solution were mixed under magnetic stirring for 1h at RT. The polymeric solutions of neat film, binary and ternary films were cast in a Teflon® mold and evaporated at RT.

Films 0.10 mm thick were obtained: the relevant material formulations are shown in **Table 1**.

**Table 1**: Material formulations for binary and ternary films

| **Formulations** | **PVA (wt%)** | **Starch NC/NP (wt%)** | **HTyr(wt%)** |
|---|---|---|---|
| **PVA** | 100 | - | - |
| **BINARY FORMULATIONS** | | | |
| **PVA/HTyr** | 95 | - | 5 |
| | | | |
| **PVA/1NC$_{WT}$** | 99 | 1 | - |
| **PVA/3NC$_{WT}$** | 97 | 3 | - |
| **PVA/1NC$_{HA}$** | 99 | 1 | - |
| **PVA/3NC$_{HA}$** | 97 | 3 | - |
| | | | |
| **PVA/1NP$_{WT}$** | 99 | 1 | - |
| **PVA/3NP$_{WT}$** | 97 | 3 | - |
| **PVA/1NP$_{HA}$** | 99 | 1 | - |
| **PVA/3NP$_{HA}$** | 97 | 3 | - |
| **TERNARY FORMULATIONS** | | | |
| **PVA/NC$_{WT}$/HTyr** | 94 | 1 | 5 |
| **PVA/NC$_{HA}$/HTyr** | 94 | 1 | 5 |
| **PVA/NP$_{WT}$/HTyr** | 94 | 1 | 5 |
| **PVA/NP$_{HA}$/HTyr** | 94 | 1 | 5 |

Different characterization methods were used to select the appropriate content of starch nanofillers, both NC and NP, to produce ternary based formulations, taking into account the final possible application in the packaging field. Thermal properties were investigated by a differential scanning calorimeter (DSC-TA Instrument, Q200), with the aim of verifying the effect of nanostructured starches on PVA crystallization phenomena and crystallinity degree. DSC measurements were performed in the temperature range from -25 to 240 °C, at a heating rate of 10 °C min$^{-1}$. Three samples were used to characterize each material.

The crystallinity degree was calculated according to the following Equation 1:

$$\chi = \frac{1}{(1-m_f)}\left[\frac{\Delta H}{\Delta H_0}\right]*100 \quad \text{(Eq. 1)}$$

where ΔH is the enthalpy for melting or crystallization; $\Delta H_0$ is enthalpy of melting for a 100% crystalline PVA sample, taken as 161.6 J $g^{-1}$ (Luzi et al., 2017; Roohani et al., 2008) and ($1-m_f$) is the weight fraction of PVA in the sample. Moreover, tensile tests of neat PVAand PVA based binary systems were performed to evaluate the effect of the nanostructured starch based fillers on the mechanical response of the PVA matrix. The test was performed on rectangular samples (50 x 10 $mm^2$) on the basis of UNI ISO 527 with a crosshead speed of 5 mm $min^{-1}$, a load cell of 500 N and an initial gauge length of 25 mm. Average tensile strength ($\sigma_B$), elongation at break ($\varepsilon_B$), and Young's modulus (E) were calculated from the resulting stress-strain curves. The measurements were done at room temperature and at least five samples for each formulation were tested.

**2.7 Characterization of ternary films**

The microstructure of the produced PVA/$NC_{WT}$/HTyr, PVA/$NC_{HA}$/HTyr, PVA/$NP_{WT}$/HTyr, PVA/$NP_{HA}$/HTyr ternary film fractured surfaces was investigated by scanning electron microscope (FESEM, Supra 25-Zeiss) after gold sputtering of the surfaces to provide enhanced conductivity and observed using an accelerating voltage of 2.5 kV. The optical properties of neat PVA and ternary films were investigated by UV-Vis spectroscopy using a Perkin Elmer Lambda 35 in the range 250-900 nm.

Thermal characterization of PVA/$NC_{WT}$/HTyr, PVA/$NC_{HA}$/HTyr, PVA/$NP_{WT}$/HTyr, PVA/$NP_{HA}$/HTyr systems was performed by both differential scanning calorimetric (DSC) and TGA. TGA (Seiko Exstar 6300) experiments were performed for each sample from 30 to 600 °C at 10 °C $min^{-1}$ under a nitrogen atmosphere (250 mL $min^{-1}$) in order to evaluate the effect of both starch fillers and HTyr addition on the thermal stability of PVA matrix. The first degradation temperature ($Td_I$), the second/maximum degradation rate temperature ($Td_{IImax}$) and its onset ($T_{onset\ main\ peak}$), the third ($Td_{III}$) and the residual mass at 600 °C were obtained from the weight loss and its derivative curves. DSC measurements were carried out on a TA Instruments DSC Q200 (TA Instruments Inc., USA) equipped with Universal Analysis 2000 software under nitrogen atmosphere in the range of -25 to 240 °C at 10 °C $min^{-1}$, carrying out two heating and one cooling scans. The glass transition temperature ($T_g$) was investigated during both heating and cooling scan; the melting

temperature and enthalpy ($T_m$ and $\Delta H_m$) were determined from the second heating scan, while crystallization temperature and enthalpy ($T_{cc}$ and $\Delta H_{cc}$) were determined from the cooling scan. The crystallinity degree was calculated according to the Equation (1).

Tensile tests of PVA/$NC_{WT}$/HTyr, PVA/$NC_{HA}$/HTyr, PVA/$NP_{WT}$/HTyr and PVA/$NP_{HA}$/HTyr films were performed at RT, as previous described, according to UNI ISO 527.

Water absorption capacity (WAC) of neat PVA and ternary films was measured on rectangular plastic probes of 10 mm x 20 mm. Specimens were first dried in a vacuum oven at 40 °C for 72 h, then cooled down in a desiccator and immediately weighted. Conditioned systems were fully immersed in a container filled with distilled water. Tests were conducted in triplicate at 4, 20 and 37 °C in order to simulate the practical condition of a packaging material. The samples were removed from the water bath at different times (1, 3, 6, and 24 h) and the surface were blotted using filter paper, and then weighed. The result of each sample represents the average of three tests.

Water absorption capacity was calculated according to the Equation (2):

$$WAC\% = (W_A - W_I)/W_I \times 100 \quad \text{(Eq. 2)}$$

where $W_A$ is the weight of the specimen at the adsorbing equilibrium and $W_I$ is the initial dry weight of the specimen.

The overall migration analysis of ternary films was also performed, in order to simulate the use of proposed package formulations with food simulant. The test was run in triplicate in simulant A (10% (v/v) ethanol water solution) according to current legislation Commission Regulation (EU) No 10/2011. Rectangular strips of 10 $cm^2$ in 10 mL of food simulant were used (European, 2011). Samples were kept in a controlled chamber at 40 °C, removed after 10 days according to EN-1186 standard, and the simulant was evaporated (European, 2002). Residues were weighed with an analytical balance (Sartorius ATILON) with ± 0.01 mg precision and the migration values in mg $kg^{-1}$ of the/each simulant were determined.

Specific migration tests were performed into ethanol 10% v/v as food simulant according to European Standard EN 13130-2005 (UNE-EN 13130–1: 2005) and European Commission Regulation 10/2011 (European, 2011). Double-sided, total immersion migration tests were carried out with 12 $cm^2$ of films and 20 mL of simulant (area-to-volume ratio around 6 $dm^2\ L^{-1}$) in triplicate at 40 ºC in an oven (J. P. Selecta, Barcelona, Spain). Samples were taken at 1, 3, 7, 10, 21 days in triplicate. A blank test for the simulant was also included. The migrated simulant was recovered after removal of samples and stored at -4 ºC before analysis.

244 **2.8 HTyr release studies in food simulant (specific migration)**

245 HTyr released by each ternary system (PVA/$NC_{WT}$/HTyr, PVA/$NC_{HA}$/HTyr, PVA/$NP_{WT}$/HTyr,
246 PVA/$NP_{HA}$/HTyr) in food simulant for every contact time (1, 3, 7, 10 and 21 days) was analyzed by
247 UV-2600 spectrophotometer (Shimadzu, Kyoto, Japan). Absorbance values were measured at
248 λ=280 nm and the concentration of the antioxidant released into the simulant was determined by a
249 calibration curve for HTyr (range: 50-400 µM) as previously described (Fortunati, Luzi, Dugo, et
250 al., 2016; Fortunati, Luzi, Fanali, et al., 2016).
251
252 **2.9 Antioxidant activity**

253 Antioxidant activities of HTyr-released from each ternary formulation were evaluated as reported
254 by Pellegrini *et al*. (Re et al., 1999) with modifications (Fortunati, Luzi, Dugo, et al., 2016;
255 Fortunati, Luzi, Fanali, et al., 2016). Briefly, the ABTS radical was generated by mixing ABTS (7
256 mM) and potassium persulfate (2.5 mM) in phosphate buffer (pH=7.4). The mixture was kept in the
257 dark overnight at room temperature. Finally, the ABTS obtained solution was diluted in ethanol in
258 order to reach an absorbance at λ=734 nm of about 0.70. A volume of 10 µl of each sample was
259 added to a 96-multiwell plate (Greiner Bio-one, Germany). The reaction was initiated by the
260 addition of 190 µL of ABTS solution. Absorbance readings were taken at λ=734 nm for 90 s in a
261 microplate reader (Infinite®, 200 Pro multimode reader, TECAN, Italy). The activity of each
262 sample was determined using Trolox as a standard (range: 50-700 µM), and the antioxidant activity
263 was expressed as Trolox Equivalent Antioxidant Capacity (TEAC). All determinations were
264 carried out in triplicate.
265
266 **3. Result and discussion**

267 **3.1. HTyr and nanostructured starch synthesis and characterization**

268 HTyr (98% pure) was synthesized on a gram scale - according to a high-yielding procedure
269 optimized by Bernini et al. (Bernini et al., 2008; Bernini et al., 2007). Granules, starch nanocrystals
270 ($NC_{WT}$, $NC_{HA}$) and starch nanoparticles ($NP_{WT}$, $NP_{HA}$) were obtained, respectively, by acid
271 hydrolysis and ultrasound irradiation of native starch extracted from WT and HA wheats. In order
272 to understand the effects of the different treatments (acid hydrolysis and ultrasound irradiation) on
273 the morphologies of native WT and HA starch, FESEM analysis was performed, by depositing a
274 drop of both native starch, starch colloid suspension after ultrasonic irradiation and starch colloid
275 suspension after acid hydrolysis, on a silicon wafer. The results, showed in **Figure 1, Panel A**

evidenced that after both acid hydrolysis (**Figure 1, Panel A c, d**) and ultrasonic treatment (**Figure 1, Panel A e, f**) the micrometric starch granules were indeed fragmented to reach nanometer size (20-50 nm). Specifically, acid hydrolysis was successfully performed and crystals with spherical shape and dimensions ranged 20-50 nm were obtained with a 4.5 and 5 of yield for WT and HA raw starch, respectively.

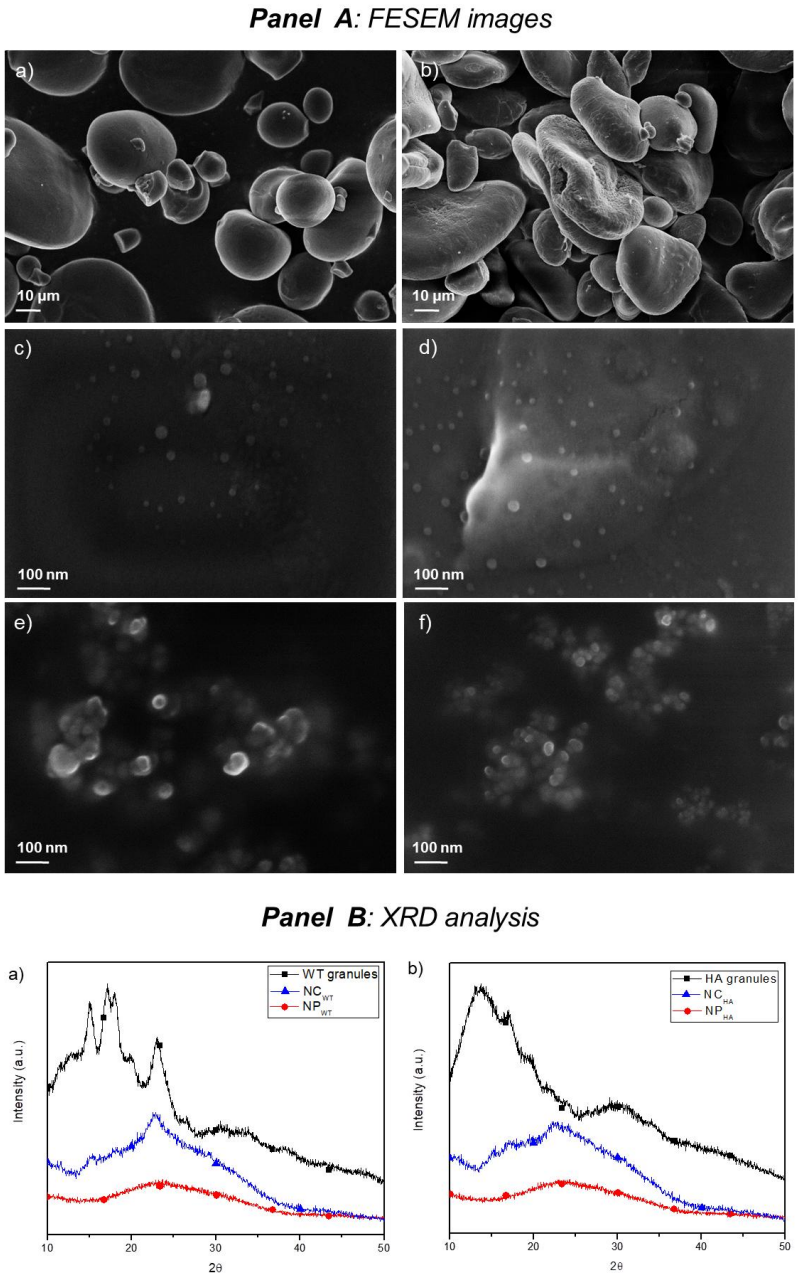


**Figure 1:** *Panel A*: FESEM images of starch particles. (a) Native WT starch; (b) native HA starch; (c) WT starch after acid hydrolysis treatment; (d) HA starch after acid hydrolysis treatment; (e) WT

starch after ultrasound treatment; (f) HA starch after ultrasound treatment. *Panel B*: XRD diffraction patterns of dried starch particles. (a) WT starch; (b) HA starch.

Concerning the ultrasound based treatment, their chemical effects on starch structure arise from acoustic cavitation, that is the formation, growth and implosive collapse of the bubbles in a liquid (Suslick, 1990). Because of the high speed, caused by bubbles collapse, the starch particles are driven together and collide violently, causing surface damage that leads to a decrease in size (Zuo, Hébraud, Hemar, & Ashokkumar, 2012).

Furthermore, X-ray diffraction was used to study the change in starch crystallinity caused by acid hydrolysis and ultrasonic treatment of WT and HA native starch. XRD diffraction patterns of dried samples of starch are shown in **Figure 1, Panel B**. As expected, the WT native starch exhibited typical diffraction pattern of cereal starch, with the peaks at Bragg angles (2θ) 15°, 17°, 18° and 23° (Zobel, H. F. (1964)) (**Figure 1, Panel B, a**). While HA native starch exhibited a different XRD spectrum due to the much higher content of amylose which resulted in a clear decrease of crystallinity (Cheetham & Tao, 1998) (**Figure 1, Panel B, b**). After acid hydrolysis both starch showed an change of crystallinity, in fact the diffraction peaks drastically decreased. While after ultrasound treatment the spectra shown a typical amorphous character. In fact, after high power ultrasound irradiation, at 8° C, acoustic cavitation causes the fragmentation of crystalline structure of clustered amylopectin leading to NPs with low crystallinity or an amorphous character (Haaj, Magnin, Pétrier, & Boufi, 2013).

### 3.2. Preparation of ternary films PVA/$NC_{WT}$/HTyr, PVA/$NC_{HA}$/HTyr, PVA/$NP_{WT}$/HTyr and PVA/$NP_{HA}$/HTyr: optimization procedure from binary systems

Binary PVA based films reinforced with 1 or 3 % wt of $NC_{HA}$ or $NC_{WT}$ and $NP_{HA}$ or $NP_{WT}$ were firstly produced, in order to select the best content of starch nanocrystals or nanoparticles to use in the ternary films. The results of the optimization procedure, conducted by performing DSC analysis and tensile tests, are summarized in **Table 2**. An evident increase in crystallinity degree values, both during the cooling and second scan ($X_c$% and $X_m$%, respectively) was induced by the presence of starch nanocrystals, that acted as nucleation agents for PVA matrix. This effect was more evident for $NC_{HA}$ based film and no significant enhancements were induced by the addition of 3 %wt of starch nanocrystals respect to the lower content (1 %wt). Moreover, the incorporation of starch nanocrystals caused an increase in Young's modulus and a consequent decrease of the elongation at

316 break of the films, that was particular evident in PVA/3$NC_{WT}$ based systems. Similar results were
317 also detected for starch nanoparticles based formulations.
318
319 **Table 2**:Thermal and mechanical properties of PVA and PVA based binary films

| | DSC | | Mechanical properties | | |
|---|---|---|---|---|---|
| **Formulations** | **$X_c$ (%)** | **$X_m$ (%)** | **$\sigma_B$ (MPa)** | **$\varepsilon_B$ (%)** | **$E_{Young}$ (MPa)** |
| **PVA** | 15.0±0.9 | 7.8±0.9 | 70±10 | 200±40 | 300±80 |
| | | | | | |
| **PVA/1$NC_{WT}$** | 23.8±1.4 | 18.2±1.3 | 51±4 | 172±9 | 647±19 |
| **PVA/3$NC_{WT}$** | 25.2±2.8 | 21.5±1.3 | 43±2 | 110±20 | 878±66 |
| **PVA/1$NC_{HA}$** | 32.0±2.2 | 28.2±2.1 | 50±5 | 135±24 | 1126±153 |
| **PVA/3$NC_{HA}$** | 36.6±0.2 | 32.8±0.2 | 52±10 | 161±35 | 1048±203 |
| | | | | | |
| **PVA/1$NP_{WT}$** | 19.6±4.1 | 11.9±2.5 | 27±6 | 152±26 | 392±34 |
| **PVA/3$NP_{WT}$** | 6.4±1.0 | 5.7±1.0 | 35±5 | 170±15 | 570±70 |
| **PVA/1$NP_{HA}$** | 21.7±0.1 | 14.3±1.7 | 29±5 | 176±5 | 301±56 |
| **PVA/3$NP_{HA}$** | 19.4±2.8 | 13.9±1.2 | 32±8 | 190±30 | 500±60 |

320
321 A general increase, although less evident respect to NC based systems, was detected for starch
322 nanoparticles based films (with the exception of PVA/3$NP_{WT}$ film) that showed a decrease of both
323 $X_c$% and $X_m$% values respect to the PVA matrix. Moreover, an increase in Young's modulus values
324 were also here detected, although less evident respect to that induced by NC in PVA matrix,
325 confirming the thermal data. Finally, starch NP were able to maintain the elongation at break values
326 of PVA matrix.
327 On the base of the previous discussed results, and taking into account the final possible application
328 of the produced formulations in packaging sector (for which barrier behaviour, directly related to
329 the crystallization characteristics and mechanical responses of the films, represent a target
330 property), the ternary nanocomposite films were prepared by adding 1% wt of $NC_{HA}$ or $NC_{WT}$ and
331 $NP_{HA}$ or $NP_{WT}$ combined with 5 %wt of active HTyr (selected on the base of our previous work
332 activity (Fortunati, Luzi, Fanali, et al., 2016) in polyvinyl alcohol matrix, by solvent casting
333 technique (see **Table 1**, Ternary film section). The obtained multifunctional formulations, about
334 0.10 mm thick, were deeply characterized.
335
336 **3.3. Characterization of ternary multifunctional nanocomposite films**
337 **3.3.1. Morphological and transparency properties**

The fractured surfaces of PVA binary films with active agent and ternary nanocomposite formulations were investigated by FESEM (**Figure 2 Panel A, a**), with the aim of evaluating the influence of both nanostructured starch (nanocrystals and nanoparticles) and active agent on PVA microstructure.

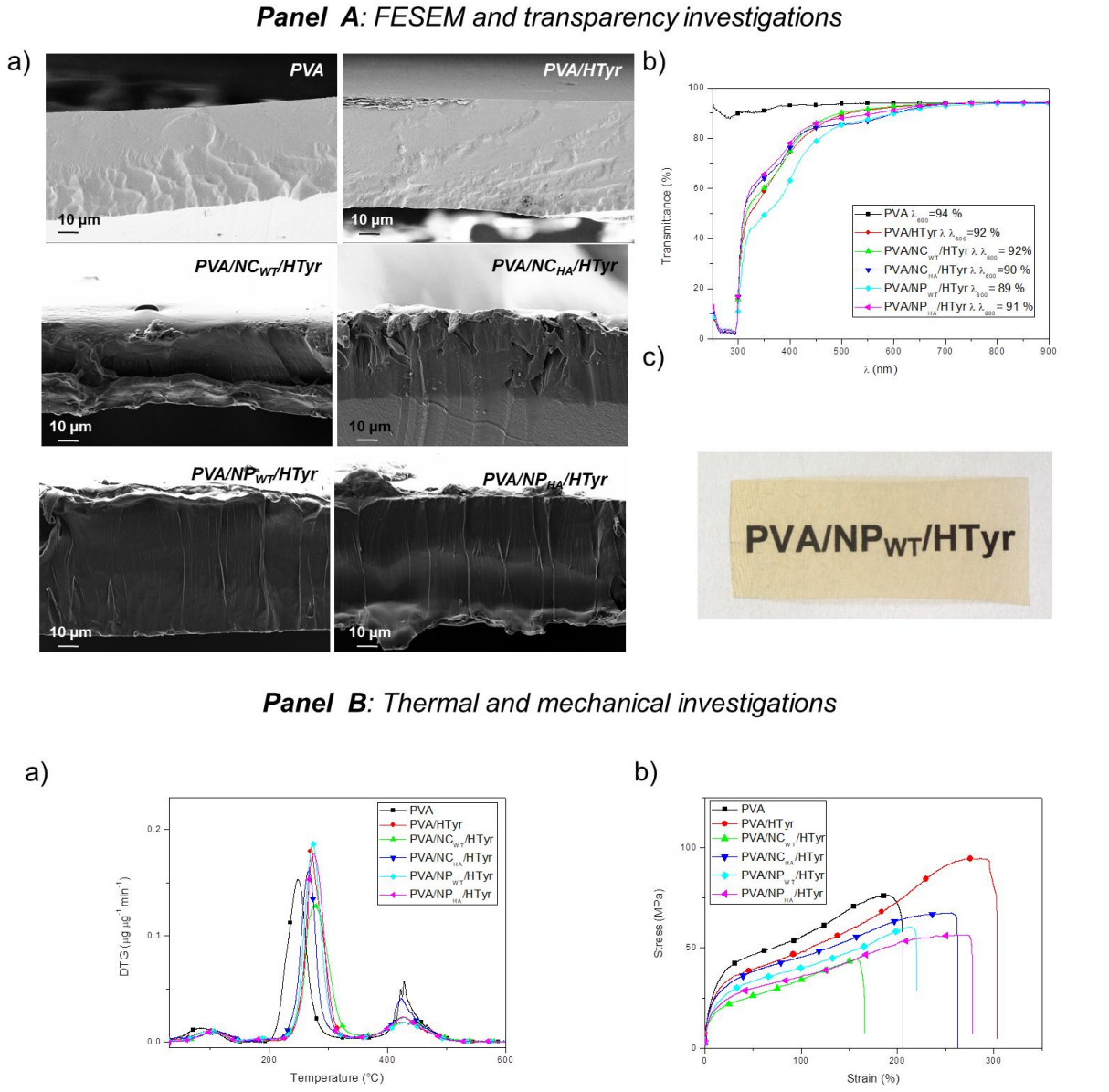


**Figure 2**: *Panel A*: FESEM investigation of fractured surface (a) and UV-Vis analysis (b) of PVA, PVA/HT$_{yr}$, PVA/NC$_{WT}$/HTyr, PVA/NC$_{HA}$/HT$_{yr}$, PVA/NP$_{WT}$/HTyr and PVA/NP$_{HA}$/HT$_{yr}$, visual image of PVA/NP$_{WT}$/HT$_{yr}$ (c). *Panel B*: derivative curves (DTG) (a) and stress-strain curves (b) of PVA, PVA/HT$_{yr}$, PVA/NC$_{WT}$/HT$_{yr}$, PVA/NC$_{HA}$/HT$_{yr}$, PVA/NP$_{WT}$/HT$_{yr}$ and PVA/NP$_{HA}$/HT$_{yr}$.

A smooth and homogeneous fractured surface was observed for neat PVA film sample. As previously reported (Fortunati, Luzi, Fanali, et al., 2016), no alterations were induced by the addition of 5 %wt of HTyr into the PVA matrix. The FESEM images underlined, in fact, no separation phases or holes, highlighting that homogeneous dispersion of the antioxidant agent in the polymeric compound was obtained and guaranteed by the solvent casting process in water.

Rougher fractured surfaces were instead observed for NC based ternary formulations, as consequence of the addition of starch nanocrystals, confirming the reinforcement effect exerted by these nanostructured fillers and confirmed by previously discussed thermal and mechanical results for NC based binary formulations. Finally, no alternations were detected for PVA/NP/HTyr based films, that showed smooth and homogeneous fractured surfaces for both $NP_{HA}$ and $NP_{WT}$ based ternary films.

Visual aspect and transparency of PVA and PVA ternary films were also analyzed. The results from UV-Vis spectra of the different produced films (**Figure 2 Panel A, b**) confirmed that the transparent nature of PVA (transmittance of 94% at a wavelength of 600 nm) was slightly affected by the addition of both active agent and nanostructured starches at this wavelength. Transmittances between 92% and 90% were, in fact, detected for PVA/HTyr binary films and all the produced ternary systems, highlighting the possibility of using these formulations to realize transparent packaging in the wavelength range of 600‑900 nm. Furthermore, the transparency behavior rapidly decreased from 600 nm to lower wavelength and all the studied systems showed a visible absorption band centered at 280 nm, due to the presence of HTyr as previously reported (Fortunati, Luzi, Fanali, et al., 2016). This different transparency vs. wavelength could modulate the employment of packaging films in different applications, in relation to specific requests, such as the increase of food shelf life, or simply to shield against a specific wavelength. Finally, visual observations (**Figure 2 Panel A, c**) confirmed the UV-Vis results, clearly showing the transparent nature of PVA based ternary films with a uniform color distribution, homogenous dispersion of the active ingredient and no significant alterations induced by the presence of nanostructured starch fillers.

### 3.3.2. Thermal analyses

Thermal properties of PVA and PVA based nanocomposite films were evaluated by differential scanning calorimetry (DSC) and thermogravimetric analysis (TGA) under nitrogen atmosphere,

with the goal of evaluating the effect of both HTyr and nanostructured starch fillers on the thermal stability of PVA matrix.

**Table 3** summarizes the values of parameters related to glass transition, crystallization and melting phenomena of PVA and PVA based ternary films, measured during the cooling and the second heating scans.

**Table 3**: DSC analysis of PVA and PVA ternary nanocomposites

| | ***Cooling*** | | | |
|---|---|---|---|---|
| ***Formulations*** | $T_g$***(°C)*** | $\Delta H_c'$***(Jg$^{-1}$)*** | $T_c'$***(°C)*** | $X_c$ ***(%)*** |
| ***PVA*** | 70.3±0.8 | 24.3±1.4 | 168.3±1.6 | 15.0±0.9 |
| ***PVA/HTyr*** | 71.2±0.6 | 51.9±1.7 | 196.1±1.8 | 30.5±1.0 |
| | | | | |
| ***PVA/NC$_{WT}$/HTyr*** | 77.6±1.0 | 52.0±2.8 | 197.0±0.3 | 32.2±1.8 |
| ***PVA/NC$_{HA}$/HTyr*** | 79.1±0.1 | 51.4±0.3 | 194.5±1.5 | 31.8±0.2 |
| ***PVA/NP$_{WT}$/HTyr*** | 75.1±0.1 | 51.4±3.3 | 197.6±0.1 | 31.8±2.0 |
| ***PVA/NP$_{HA}$/HTyr*** | 77.3±1.6 | 53.0±0.6 | 197.4±1.6 | 32.8±0.4 |
| | ***Second heating*** | | | |
| | $T_g$***(°C)*** | $\Delta H_m$***(Jg$^{-1}$)*** | $T_m$ ***(°C)*** | $X_m$***(%)*** |
| ***PVA*** | 84.1±1.2 | 12.6±1.5 | 206.1±3.4 | 7.8±0.9 |
| ***PVA/HTyr*** | 79.9±1.1 | 46.5±2.6 | 222.1±1.1 | 27.3±1.5 |
| | | | | |
| ***PVA/NC$_{WT}$/HTyr*** | 81.3± 0.1 | 57.7±1.0 | 225.1±0.2 | 35.7±0.6 |
| ***PVA/NC$_{HA}$/HTyr*** | 80.7±0.3 | 55.2±0.3 | 223.7±0.8 | 34.1±0.2 |
| ***PVA/NP$_{WT}$/HTyr*** | 79.3±1.9 | 58.1±0.4 | 226.2±2.0 | 36.0±0.2 |
| ***PVA/NP$_{HA}$/HTyr*** | 80.2±0.6 | 52.1±3.6 | 225.1±1.3 | 32.3±2.2 |

The incorporation of NC and NP combined with HTyr induced a change in the thermal properties of the different PVA based formulations produced by solvent casting. A slight increase in term of glass transition temperature ($T_g$) was registered in PVA/NC/HTyr and PVA/NP/HTyr based films in the cooling scan respect to PVA and PVA/HTyr, while no particular variation in terms of $T_g$ were observed during the second heating scan. As previously reported in literature, the presence of HTyr favors the crystallization phenomena of PVA/HTyr (Fortunati, Luzi, Fanali, et al., 2016). The crystallinity degree in ternary films increased both during the cooling and second heating scan ($X_c$% and $X_m$%, respectively) as a consequence of the increase in enthalpy values, this phenomenon was previously observed in binary films PVA/NC and PVA/NC based films (**Table 2**). However, the

combination of HTyr and starch nanofiller in PVA matrix did not induce a proportional increase in term of enthalpy, and consequently in terms of crystallinity degree, during cooling and second heating scans. This phenomenon was also confirmed by the observation of crystallization and melting temperature values. A significant shift of about 15–20 °C of the crystallization temperatures ($T_c$) to higher values was registered for PVA/HTyr respect to the neat PVA ($T_c$= 168.3 ± 1.6 °C), the combination of active ingredient and starch nanostructure didn't determine a significant increase of this parameter. An increase of the $\Delta H_c$ of about 20--25 (J $g^{-1}$) was registered adding HTyr in PVA matrix, while no variation of $\Delta H_c$ was registered combining HTyr and starch nanostructures respect to PVA/HTyr. A similar behavior was also observed for the melting phenomena occurring during the second heating scan. The melting temperatures and enthalpies ($T_m$ and $\Delta H_m$) did not increase, in fact, proportionally combining HTyr and NC or NP in the polymer matrix (**Table 3**).

The effect of the different additives on the thermal degradative properties of PVA matrix was also investigated by TGA, derivative curves of weight loss are reported in **Figure 2 Panel B, a**. All the studied formulations were characterized by the presence of a multi-step degradation behavior. The first weight loss, at low temperature centered at around 80‑110 °C, corresponds to the evaporation of the water or a weight loss of low molecular weight compounds (Fortunati et al., 2013). The second and the third degradation temperatures correspond to the degradation of neat PVA (Fortunati et al., 2013; Frone et al., 2011; Thomas, Guerbois, Russell, & Briscoe, 2001). In particular, the second/main degradation step of PVA film corresponds to the removal of residual acetate groups, due to the incomplete hydrolysis of PVA that remains in the chains (Li, Yue, & Liu, 2012). It was previously reported, and here confirmed, that the presence of HTyr in the PVA matrix shifted the main degradation temperature to higher values, whereas no alterations in the main degradation temperatures were induced by the presence of different nanostructured starch fillers. Finally, the third degradation step, due to the cyclization reaction and continual elimination of residual acetate groups (Lu, Wilkie, Ding, & Song, 2011), was poorly affected by the presence of both HTyr and starch nanofillers (Fortunati, Luzi, Fanali, et al., 2016).

### 3.3.3. Mechanical response

The results from tensile test for PVA and PVA ternary nanocomposite formulations are summarized in **Table 4**, whereas **Figure 2, Panel B, b** reports the characteristics stress-strain curves for all the studied films. PVA neat films showed an elongation at break around (200 ± 40)%, confirming the ductile nature of the selected polymer matrix (Kavoosi, Nateghpoor, Dadfar, & Dadfar, 2014; Peng

& Kong, 2007). The addition of 5 %wt of HTyr to PVA induced an increase of about 150% respect to PVA matrix, underlining and confirming the plasticization effect of the selected active ingredient.

**Table 4**: Mechanical properties of PVA and PVA ternary nanocomposites

| Formulations | $\sigma_B$ (MPa) | $\varepsilon_B$ (%) | $E_{Young}$ (MPa) |
|---|---|---|---|
| **PVA** | 70±10 | 200±40 | 300±80 |
| **PVA/HTyr** | 80±15 | 300±50 | 300±50 |
| | | | |
| **PVA/$NC_{WT}$/HTyr** | 60±8 | 195±20 | 455±55 |
| **PVA/$NC_{HA}$/HTyr** | 64±8 | 248±19 | 480±37 |
| **PVA/$NP_{WT}$/HTyr** | 60±6 | 232±24 | 397±36 |
| **PVA/$NP_{HA}$/HTyr** | 60±4 | 265±18 | 382±36 |

This effect was, in part, maintained also in the case of ternary systems, that showed elongation at break values higher than 230-250%, with the exception of PVA/$NC_{WT}$/HTyr films, that revealed the lowest value of elongation (195 ± 20) %. Moreover, highest values of elongation at break were guaranteed by NP respect to NC. These data were also confirmed by the trend registered for Young's modulus values. All the produced ternary formulations showed Young's modulus values higher than neat PVA film, highlighting, as expected, the reinforcement effect exerted by the selected nanostructured fillers. However, the highest values of Young's modulus were detected for starch nanocrystal based films, featuring the reinforcement effect of this filler respect to the starch nanoparticles.

### 3.3.4. Water absorption capacity

In order to evaluate the effect of different components and their combinations in the polymer matrix, water absorption capacity (WAC) of PVA based formulations combined with starch nanofillers and hydroxytyrol was investigated at 4, 20, and 37 °C (**Table 5**). Three different temperatures (4, 20, and 37 °C) were selected, in order to reproduce and simulate the different thermal conditions to which the food products are exposed during the transport and the storage. All the produced and studied formulations (PVA, PVA/HTyr, PVA/$NC_{WT}$/HTyr, PVA/$NC_{HA}$/HTyr, PVA/$NP_{WT}$/HTyr and PVA/$NP_{HA}$/HTyr) showed a fast absorption mechanism with a saturation limit reached within the first 24 h for all the samples (Fortunati, Luzi, Dugo, et al., 2016; Elena Fortunati, Luzi, Fanali, et al., 2016), due to the hydrophilic nature of the polymer matrix that

justifies this behaviour (Cano, Cháfer, Chiralt, & González-Martínez, 2016; Fortunati et al., 2013; Kavoosi et al., 2014).

**Table 5**: Water absorption capacity of PVA and PVA based films after 24 h of incubation in water at 4 °C, 20 °C and 37 °C and overall migration values for different formulations.

| Formulations | WAC (%) after 24 h | | | Overall Migration |
|---|---|---|---|---|
| | 4 °C | 20 °C | 37 °C | in ethanol 10 (v/v)% (mg $kg^{-1}$) |
| **PVA** | 235.7 ± 5.9 | 282.8±4.3 | 336.6±26.6 | 2.4±0.1 |
| **PVA/HTyr** | 200.0±26.7 | 258.6±10.0 | 244.7±15.6 | 2.5±0.1 |
| | | | | |
| **PVA/$NC_{WT}$/HTyr** | 315.6±2.1 | 363.3±28.9 | 332.1±29.3 | 3.3±0.1 |
| **PVA/$NC_{HA}$/HTyr** | 284.7±16.3 | 334.5±12.8 | 321.8±0.2 | 3.5±0.1 |
| **PVA/$NP_{WT}$/HTyr** | 320.5±12.0 | 418.2±15.0 | 377.3±11.5 | 3.4±0.1 |
| **PVA/$NP_{HA}$/HTyr** | 277.1±13.0 | 325.4±13.8 | 324.4±15.6 | 3.5±0.2 |

The WAC % for PVA film, and generally for PVA based formulations, was higher at 37 °C (**Table 5**), being related to temperature effect on polymer chain mobility. The temperature at 37 °C is closer to the glass transition temperature of the PVA based film ($T_g$ =70.3±0.8 °C). Finally, in PVA ternary based films, the presence of starch nanofillers influence the WAC%, specifically their presence determined an increase of swelling phenomena, due to the hydrophilic nature of PVA and starch nanostructures (Cano et al., 2016; Fortunati et al., 2013; Luzi et al., 2017). Finally, verifying the data obtained from ternary based formulations, it is possible to observe that no particular differences were experimentally obtained by using NC or NP (**Table 5**) in the polymer matrix in terms of WAC % at different temperature of test. A slight increase in terms of WAC% were registered only in the case of PVA ternary based films combined with NC or NP extracted from WT starch granules. It is widely known that the increase in amylose limits the water absorbtion capacity of starch due to the tight interaction among its linear glycosidic chains (Graner, and Frison, 2014; Sestili, Botticella, & Lafiandra, 2014)

### 3.3.5. Overall migration and release tests in food simulant

Overall migration tests with food simulant of PVA ternary formulations were performed on the base of European Union Regulation no. 10/2011, which defines the limits at which additives can migrate into food during the storage, transport and commercialization period of foodstuff. The results are summarized in **Table 5**. The migrated values for all the studied formulations were lower than the

migration limits for food contact materials, 60 mg $kg^{-1}$ simulant, established by the current European legislation (European, 2011), demonstrating the possible practical application of the produced films in contact with the foods. Release tests were performed according to European Standard EN 13130-200522 and European Commission Regulation 10/2011 (European, 2011). Each formulation (PVA/$NC_{WT}$/HTyr, PVA/$NC_{HA}$/HTyr, PVA/$NP_{WT}$/HTyr, PVA/$NP_{HA}$/HTyr) was placed into the simulant for water-based foods (ethanol 10% v/v) for 21 days. All samples were analyzed at 1, 3, 7, 10 and 21 days in terms of HTyr release (**Figure 3, a**).

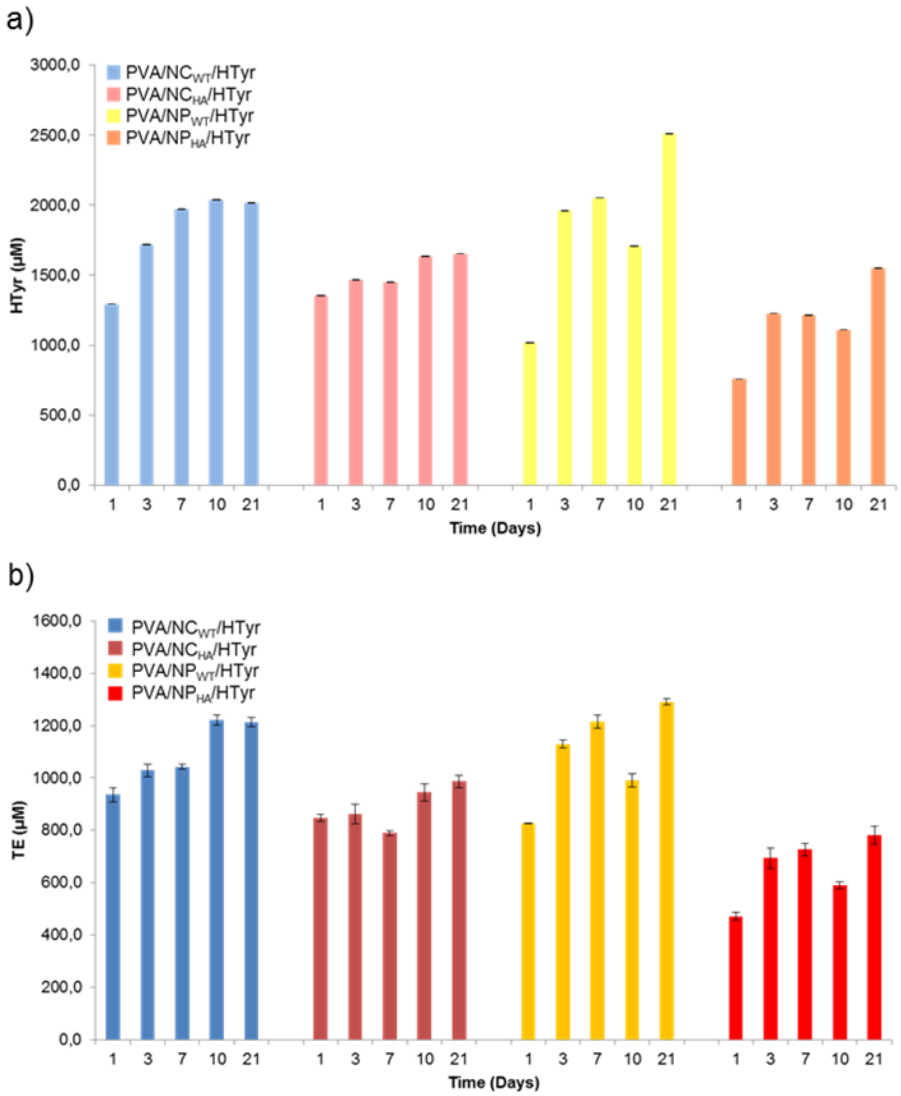


**Figure 3**: HTyr released from the ternary films PVA/$NC_{WT}$/HTyr, PVA/$NC_{HA}$/HTyr, PVA/$NP_{WT}$/$HT_{yr}$, PVA/$NP_{HA}$/$HT_{yr}$ in food simulant (expressed as µM) (a); antioxidant activity of food simulant solutions after specific migration tests of ternary films PVA/$NC_{WT}$/$HT_{yr}$

507 $PVA/NC_{HA}/HT_{yr}$ $PVA/NP_{WT}/HT_{yr}$ $PVA/NP_{HA}/HT_{yr}$ evaluated by ABTS assay and expressed as
508 Trolox Equivalents (TE, μM) (b).
509
510 As showed in **Figure 3, a**, each formulation allowed a controlled-HTyr release during the 21 days.
511 In fact, an increasing trend of HTyr released was observed for all formulations reaching the
512 maximum value at day 21. In particular, HTyr concentrations in the stimulant solutions ranged from
513 756.41 μM when released from $PVA/NP_{HA}$/HTyr, to 1351.28 μM from $PVA/NC_{HA}$/HTyr at day 1
514 and from 1549.35 μM for $PVA/NP_{HA}$/HTyr to 2511.53 μM from $PVA/NP_{WT}$/HTyr at day 21.
515 Among all formulations, $PVA/NP_{WT}$/HTyr resulted the most efficient, guaranteeing a progressive
516 HTyr release during the 21 days of the test.
517
518 **3.3.5. Antioxidant activity**
519 The antioxidant activity of the ternary formulations $PVA/NC_{WT}$/HTyr, $PVA/NC_{HA}$/HTyr,
520 $PVA/NP_{WT}$/HTyr, $PVA/NP_{HA}$/HTyr was evaluated at different times (1, 3, 7, 10 and 21 days), in
521 details the food simulant solutions previously tested for the specific migration were subjected to the
522 ABTS assay. The experimental data, showed in **Figure 3,b**, confirmed that all samples exhibited a
523 remarkable antioxidant activity. In addition, the effect of the different formulations was in
524 agreement with the experimental data of the specific migration. In fact, the antioxidant activity
525 increased during the 21 days, ranging from 471.30 μM for $PVA/NP_{HA}$/HTyr to 935.46 μM for
526 $PVA/NC_{WT}$/HTyr at day 1, and from 780.74 μM ($PVA/NP_{HA}$/HTyr) to 1291.21 μM for
527 $PVA/NP_{WT}$/HTyr at day 21.
528
529 **4. Conclusions**
530 Experimental data reported in this paper give a solid evidence that ternary films based on PVA,
531 nanostructured starch and a strong antioxidant compound such as HTyr, represent very promising
532 novel combinations for active food packaging applications. HTyr was released in the food simulant
533 in a controlled manner from all films and the resulting solution exhibited the antioxidant activity all
534 along the 21 days of the test. These release profiles confirmed the hypothesis that nanostructured
535 starch-based formulations were able to tune the release of HTyr from the films over the time.
536 Among all films, $PVA/NP_{WT}$/HTyr showed the most efficient and sustained release of HTyr and as
537 consequence also the related antioxidant capacity on food simulant.
538

**Acknowledgments**

Authors are grateful to Prof. Laura Dugo (University Campus Bio-Medico, Rome, Italy) for the training on the evaluation of the antioxidant activity by the ABTS method and her willingness to discuss the experimental data.

**References**

Acevedo-Fani, A., Soliva-Fortuny, R., & Martín-Belloso, O. (2016). Nanostructured emulsions and nanolaminates for delivery of active ingredients: improving food safety and functionality. Trends in *Food Science & Technology, 60,* 12-22.

Agustin-Salazar, S., Gamez-Meza, N., Medina-Juàrez, L. À., Soto-Valdez, H., & Cerruti, P. (2014). From Nutraceutics to Materials: Effect of Resveratrol on the Stability of Polylactide. *ACS Sustainable Chemistry & Engineering, 2(6),* 1534-1542.

Ambrogi, V., Cerruti, P., Carfagna, C., Malinconico, M., Marturano, V., Perrotti, M., & Persico, P. (2011). Natural antioxidants for polypropylene stabilization. *Polymer Degradation and Stability*, 96(12), 2152-2158.

Angellier, H., Choisnard, L., Molina-Boisseau, S., Ozil, P., & Dufresne, A. (2004). Optimization of the preparation of aqueous suspensions of waxy maize starch nanocrystals using a response surface methodology. *Biomacromolecul*es, 5(4), 1545-1551.

Bernini, R., Carastro, I., Palmini, G., Tanini, A., Zonefrati, R., Pinelli, P., Brandi, M.L., Romani, A. Romani, A. (2017). Lipophilization of Hydroxytyrosol-Enriched Fractions from Olea europaea L. Byproducts and Evaluation of the in Vitro Effects on a Model of Colorectal Cancer Cells. *Journal of Agricultural and Food Chemistry, 65(31),* 6506-6512.

Bernini, R., Gilardini Montani, M. S., Merendino, N., Romani, A., & Velotti, F. (2015). Hydroxytyrosol-Derived Compounds: A Basis for the Creation of New Pharmacological Agents for Cancer Prevention and Therapy. *Journal of medicinal chemistry, 58,* 9089–9107 .

Bernini, R., Merendino, N., Romani, A., & Velotti, F. (2013). Naturally occurring hydroxytyrosol: synthesis and anticancer potential. *Current medicinal chemistry, 20(5),* 655-670.

Bernini, R., Mincione, E., Barontini, M., & Crisante, F. (2008). Convenient synthesis of hydroxytyrosol and its lipophilic derivatives from tyrosol or homovanillyl alcohol. *Journal of agricultural and food chemistry, 56(19),* 8897-8904.

570 Bernini, R., Mincione, E., Crisante, F., Barontini, M., Fabrizi, G., & Gentili, P. (2007).
571 Chemoselective and efficient carbomethoxylation of the alcoholic chain of phenols by dimethyl
572 carbonate (DMC). *Tetrahedron Letters, 48(39)*, 7000-7003.
573 Botticella; E.; Sestili, F.; Sparla, F.; Moscatello, S.; Marri, L.; Cuesta-Seijo, J. A.; Falini, G.;
574 Battistelli, A.; Trost, P.; Lafiandra, D Combining mutations at genes encoding key enzymes
575 involved in starch synthesis affects the amylose content, carbohydrate allocation and hardness in the
576 wheat grain. *Plant Biotech*. J. submitted
577 Cano, A., Cháfer, M., Chiralt, A., & González-Martínez, C. (2016). Development and
578 characterization of active films based on starch-PVA, containing silver nanoparticles. *Food*
579 *Packaging and Shelf Life, 10*, 16-24.
580 Castro López, M. d. M., López de Dicastillo, C., López Vilariño, J. M., & González Rodríguez, M.
581 V. (2013). Improving the Capacity of Polypropylene To Be Used in Antioxidant Active Films:
582 Incorporation of Plasticizer and Natural Antioxidants. *Journal of Agricultural and Food Chemistry,*
583 *61(35)*, 8462-8470.
584 Cerruti, P., Malinconico, M., Rychly, J., Matisova-Rychla, L., & Carfagna, C. (2009). Effect of
585 natural antioxidants on the stability of polypropylene films. *Polymer Degradation and Stability,*
586 *94(11)*, 2095-2100.
587 Cheetham, N. W. H., & Tao, L. (1998). Variation in crystalline type with amylose content in maize
588 starch granules: an X-ray powder diffraction study. *Carbohydrate polymers, 36(4)*, 277-284.
589 Domingues, R. M. A., Silva, M., Gershovich, P., Betta, S., Babo, P., Caridade, S. G., Mano, J.F.,
590 Motta, A., Reis, R.L., Gomes, M. E. (2015). Development of Injectable Hyaluronic Acid/Cellulose
591 Nanocrystals Bionanocomposite Hydrogels for Tissue Engineering Applications. *Bioconjugate*
592 *Chemistry, 26(8)*, 1571-1581.
593 European, C. (2011). Commission Regulation (EU) No. 10/2011 of 14 January 2011 on plastic
594 materials and articles intended to come into contact with food. Off J Eur Comm, 50, 1-89.
595 European Standard EN 1186–1: 2002−. Materials and articles in contact with foodstuff s. Plastics.
596 Guide to the selection of conditions and test methods for overall migration.).
597 Fortunati, E., Luzi, F., Dugo, L., Fanali, C., Tripodo, G., Santi, L., Kenny, J.M., Torre, L., Bernini,
598 R. (2016). Effect of hydroxytyrosol methyl carbonate on the thermal, migration and antioxidant
599 properties of PVA- based films for active food packaging. *Polymer International, 65 (8),* 872-882.

600 Fortunati, E., Luzi, F., Fanali, C., Dugo, L., Belluomo, M. G., Torre, L., Kenny, J.M., Santi, L.,
601 Bernini, R. (2016). Hydroxytyrosol as Active Ingredient in Poly (vinyl alcohol) Films for Food
602 Packaging Applications. *Journal of Renewable Materials, 5(2),* 81-95.
603 Fortunati, E., Puglia, D., Luzi, F., Santulli, C., Kenny, J. M., & Torre, L. (2013). Binary PVA bio-
604 nanocomposites containing cellulose nanocrystals extracted from different natural sources: Part I.
605 *Carbohydrate Polymers, 97(2),* 825-836.
606 Frone, A. N., Panaitescu, D. M., Donescu, D., Spataru, C. I., Radovici, C., Trusca, R., & Somoghi,
607 R. (2011). Preparation and characterization of PVA composites with cellulose nanofibers obtained
608 by ultrasonication. *BioResources, 6(1),* 487-512.
609 Gambacorta, A., Tofani, D., Bernini, R., & Migliorini, A. (2007). High-Yielding Preparation of a
610 Stable Precursor of Hydroxytyrosol by Total Synthesis and from the Natural Glycoside Oleuropein.
611 J*ournal of Agricultural and Food Chemistry, 55(9),* 3386-3391.
612 Graner, A., &E. Frison, E. (2014) editors, Genomics of plant genetic resources. Springer
613 Netherlands, Dordrecht. p. 467–487.)
614 Haaj, S. B., Magnin, A., Pétrier, C., & Boufi, S. (2013). Starch nanoparticles formation via high
615 power ultrasonication. *Carbohydrate polymers, 92(2),* 1625-1632.
616 Kavoosi, G., Nateghpoor, B., Dadfar, S. M. M., & Dadfar, S. M. A. (2014). Antioxidant, antifungal,
617 water binding, and mechanical properties of poly (vinyl alcohol) film incorporated with essential oil
618 as a potential wound dressing material. *Journal of Applied Polymer Science, 131(20).*
619 LeCorre, D., Bras, J., & Dufresne, A. (2011). Influence of botanic origin and amylose content on
620 the morphology of starch nanocrystals. *Journal of Nanoparticle Research, 13(12),* 7193-7208.
621 Lee, S. Y., Lee, S. J., Choi, D. S., & Hur, S. J. (2015). Current topics in active and intelligent food
622 packaging for preservation of fresh foods. *Journal of the Science of Food and Agriculture, 95(14),*
623 2799-2810.
624 Li, W., Yue, J., & Liu, S. (2012). Preparation of nanocrystalline cellulose via ultrasound and its
625 reinforcement capability for poly (vinyl alcohol) composites. *Ultrasonics sonochemistry, 19(3),*
626 479-485.
627 Lu, H., Wilkie, C. A., Ding, M., & Song, L. (2011). Thermal properties and flammability
628 performance of poly (vinyl alcohol)/α-zirconium phosphate nanocomposites. *Polymer Degradation*
629 *and Stability, 96(5),* 885-891.
630 Luzi, F., Fortunati, E., Giovanale, G., Mazzaglia, A., Torre, L., & Balestra, G. M. (2017). Cellulose
631 nanocrystals from Actinidia deliciosa pruning residues combined with carvacrol in PVA_CH films

632 with antioxidant/antimicrobial properties for packaging applications. *International Journal of*
633 *Biological Macromolecules, 104*, 43-55.
634 Luzi, F., Fortunati, E., Jiménez, A., Puglia, D., Pezzolla, D., Gigliotti, G., Kenny, J.M., Chiralt, A.,
635 & Torre, L. (2016). Production and characterization of PLA_PBS biodegradable blends reinforced
636 with cellulose nanocrystals extracted from hemp fibres. *Industrial Crops and Products, 93(25)*,
637 276-289.
638 Peng, Z., & Kong, L. X. (2007). A thermal degradation mechanism of polyvinyl alcohol/silica
639 nanocomposites. *Polymer degradation and stability, 92(6)*, 1061-1071.
640 Re, R., Pellegrini, N., Proteggente, A., Pannala, A., Yang, M., & Rice-Evans, C. (1999).
641 Antioxidant activity applying an improved ABTS radical cation decolorization assay. *Free radical*
642 *biology and medicine, 26(9)*, 1231-1237.
643 Romani, A., Pinelli, P., Ieri, F., & Bernini, R. (2016). Sustainability, Innovation, and Green
644 Chemistry in the Production and Valorization of Phenolic Extracts from Olea europaea L.
645 *Sustainability, 8(10)*, 1002; doi:10.3390/su8101002.
646 Roohani, M., Habibi, Y., Belgacem, N. M., Ebrahim, G., Karimi, A. N., & Dufresne, A. (2008).
647 Cellulose whiskers reinforced polyvinyl alcohol copolymers nanocomposites. *European polymer*
648 *Journal, 44(8)*, 2489-2498.
649 Sestili, F., Botticella, E., & Lafiandra, D. (2014). TILLING for improved starch composition in
650 wheat. In Genomics of Plant Genetic Resources (pp. 467-487): Springer
651 Siró, I., Fenyvesi, É., Szente, L., De Meulenaer, B., Devlieghere, F., Orgoványi, J., Sényi, J., Barta,
652 J. (2006). Release of alpha-tocopherol from antioxidative low-density polyethylene film into fatty
653 food simulant: influence of complexation in beta-cyclodextrin. *Food additives and contaminants,*
654 *23(8)*, 845-853.
655 Stark, W. J., Stoessel, P. R., Wohlleben, W., & Hafner, A. (2015). Industrial applications of
656 nanoparticles. *Chemical Society Reviews, 44(16)*, 5793-5805.
657 Suslick, K. S. (1990). Sonochemistry. *Science, 247(4949)*, 1439-1446.
658 Thomas, P. S., Guerbois, J. P., Russell, G. F., & Briscoe, B. J. (2001). FTIR study of the thermal
659 degradation of poly (vinyl alcohol). *Journal of thermal analysis and calorimetry, 64(2)*, 501-508.
660 UNE-EN 13130-1:2005, Materials and articles in contact with foodstuffs. Plastics substances
661 subject to limitation. Guide to test methods for the specific migration of substances from plastics to
662 foods and food simulants and the determination of substances in plastics and the selection of
663 conditions of exposure to food simulants (2005).

Wang, Y., Zhao, Q., Han, N., Bai, L., Li, J., Liu, J., Che, E., Hu L., Zhang Q., Jiang T., & Wang, S. (2015). Mesoporous silica nanoparticles in drug delivery and biomedical applications. *Nanomedicine: Nanotechnology, Biology and Medicine, 11(2),* 313-327.

Wolf, M. (1964). Wheat starch. In R. Whistler (Ed.), Methods in carbohydrate chemistry. Academic press New York, pages 6-9.).

Zobel, H. F. (1964). X-ray analysis of starch granules. In L. R. Whistler, & R. J. Smith (Eds.), Methods in carbohydrate chemistry (pp. 109-113). New York: Academic press)

Zuo, Y. Y. J., Hébraud, P., Hemar, Y., & Ashokkumar, M. (2012). Quantification of high-power ultrasound induced damage on potato starch granules using light microscopy. *Ultrasonics Sonochemistry, 19(3),* 421-426.

696 **Graphical abstract**

697

698